

The Calculation of Local Magnitude from the Simulated Wood-Anderson Seismograms of the Short-Period Seismograms in the Taiwan Area

TZAY-CHYN SHIN¹

(Manuscript received 10 December 1992, in final form 24 April 1993)

ABSTRACT

The attenuation function, $\log A_o(\Delta)$, used in the calculation of local magnitude is derived for the Taiwan area. The simulated Wood-Anderson seismograms are constructed by using digital three-components short-period seismogram of the Central Weather Bureau Seismic Network, (CWBSN). The decay of peak amplitude with distance is the attenuation characteristic of seismic energy. Also, it essentially represents the distance correction term, $\log A_o(\Delta)$, after a proper normalization. Considering the focal depth of earthquakes in the Taiwan area, the $\log A_o(\Delta)$ functions are:

$$\log A_o(\Delta) = \begin{cases} -0.00716R - \log R - 0.39 & (0 \text{ km} < \Delta \leq 80 \text{ km}) \\ -0.00261R - 0.83 \log R - 1.07 & (80 \text{ km} < \Delta) \end{cases}$$

for shallow earthquakes (focal depth, $h \leq 35$ km) and

$$\log A_o(\Delta) = -0.00326R - 0.83 \log R - 1.01$$

for deep earthquakes ($h > 35$ km)

where Δ is epicentral distance, $R(= \sqrt{\Delta^2 + h^2})$ is the hypocentral distance. Results also show that the local magnitude of a deep earthquake is underestimated by using the Richter's $\log A_o(\Delta)$ values (1935, 1958) with comparison to the M_L value obtained from the revised $\log A_o(\Delta)$ values of this study. By applying the revised attenuation function, a compatible local magnitude can be calculated from the strong motion data.

The conversion of duration magnitude, M_D which is currently used in the Taiwan area, to M_L is in the form:

$$M_L = 1.12M_D + 0.03 \pm 0.21$$

¹ Central Weather Bureau, 64, Kung Yuan Road, Taipei, Taiwan, R.O.C.

1. INTRODUCTION

The local magnitude, M_L , popularly used by local seismic network was formulated by Richter (1935, 1958) as :

$$M_L = \log A - \log A_o(\Delta) \quad (1)$$

where A is the maximum amplitude in millimeters recorded on the standard Wood-Anderson torsion seismograph with static magnification of 2800, natural period of 0.8 second, and damping factor of 0.8 at an epicentral distance Δ , A_o which describes the loss of energy with respect to distance such as geometrical spreading, anelastic attenuation, and wave scattering is distant dependent. These effects depend on the characteristics of the crust and upper mantle of applied area. The $\log A_o$ function is of more interesting in engineering seismology and seismology.

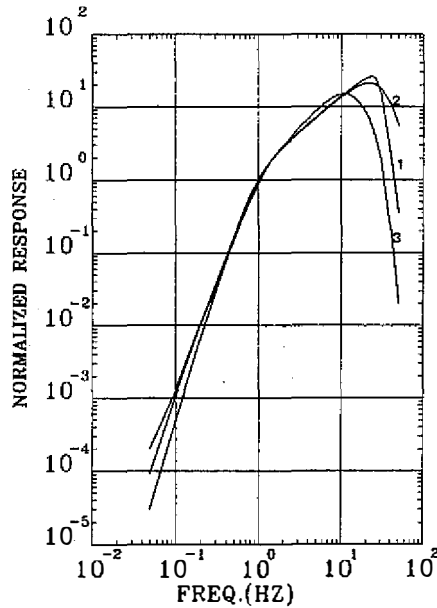
The M_L formulation was originally designed for the region of southern California where the function of $\log A_o(\Delta)$ was empirically determined. However, equation (1) is also used in the other seismic network to determined local magnitude as the Richter's southern California $\log A_o$ is used with the assumption of similar characteristics of the crust and upper mantle. On the other hand, a number of studies (Yeh *et al.*, 1982; Bakun and Joyner, 1984; Chavoz and Priestley, 1985), reconstructed the $\log A_o$ function for the applied area by using synthetic Wood-Anderson seismogram from strong motion or short period seismogram.

In this paper, I use short period digital seismograms to simulate Wood-Anderson seismograms. To study the attenuation of seismic wave, a new $\log A_o(\Delta)$ curve can be developed for Taiwan area and calibrated so that $\log A_o(100) = -3$. The variety of $\log A_o(\Delta)$ for earthquake occurring at different focal depths is taken into account. It is due to the wide range of focal depths in Taiwan area. This gives less Lg wave excitation (Campillo *et al.* 1983) for earthquake occurring beneath the crust.

2. DATA

Since 1991, the Central Weather Bureau (CWB) has upgraded the seismic network, named as Central Weather Bureau Seismic Network (CWBSN). The local station of new system is installed with a three-component short-period digital seismographs while a real-time operation is performed in the center. The seismograph is the velocity type sensor, S13, and has adjustable natural frequency of from 0.75 Hz to 1.1 Hz. The signal is digitized locally by a 12-bit A/D converter with 100 samples per second, and then transmitted through the dedicated phone line of 4800 baud rate. The network consists of 68 stations, including 43 digital stations belonging to the CWB and 25 one-component short-period stations of the Taiwan Telemetered Seismograph Network (TTSN), which is operated by the Institute of Earth Sciences (IES), Academia Sinica since 1973. The telemetry of TTSN is analog transmission. The signal is digitized with the same sample rate as CWB's signal at the center of CWBSN. The system is well calibrated by using weight lift and 1 Hz harmonic current feed technique. The normalized instrument responses for three instrumental type are shown in Figure 1. The sensitivity factor as well as station parameters are listed in Table 1. The last column of Table 1 is the instrumental type : 1 for S-13 sensor with analog transmission; 2 for L-4C sensor with analog transmission; 3 for S-13 sensor with digital transmission whose response curves are shown in Figure 1.

Fig. 1. Normalized instrument responses. The number written near by curve denotes the instrument type as listed in the last column of Table 1.



At each of the 43 digital stations, a strong motion accelerograph, A800 (Teledyne), is also installed. The instrument is a triggered type and the triggered level is generally set up at 2% of the full scale (1g). The local accelerograph is connected to dial-up phone line for data retrieval, calibration, and timing synchronization.

The current local magnitude is calculated from the simulated Wood-Anderson seismogram from the short-period digital seismogram while the Richter's $\log A_0(\Delta)$ curve (1935, 1958) is used. The uncertainty of local magnitude may be caused by the use of $\log A_0(\Delta)$ which is essentially valid for southern California. Moreover, the Richter's $\log A_0(\Delta)$ function (1935, 1958) is of depth-independence since almost all earthquakes in southern California are shallow. But, it is not so for earthquakes in Taiwan.

In order to derive a proper $\log A_0(\Delta)$ function which is suitable for the Taiwan area, the ray path of selected earthquakes should be able to sample the whole area. Totally, 224 earthquakes occurring in the period of Sept. 1991 to Feb. 1992 with wide range of focal depth from shallow to 120 km are selected in this study on the basis of the following criteria: (1) The event was recorded by at least 10 digital stations, without clipped amplitude (2048 counts) on horizontal components; and (2) The distance from the nearest station to the farthest one under condition (1) must be greater than 150 km. Figure 2 is a location map to show all events used in this study.

3. DATA ANALYSIS AND RESULTS

The value of the amplitude of seismic wave at epicentral distance Δ , denoted as $A(\Delta)$, is the combined results of material attenuation and geometrical spreading. The $A(\Delta)$ can be written as

$$A(\Delta) = C e^{-\gamma R} / R^n S \quad (2)$$

Table 1. The stations parameters of CWBSN.

Station Code	Latitude Degree	Longitude Degree	Gain (count/mu)	Instrument Type*
TAP	25.04	121.52	.013	3
HSN	24.80	120.97	.013	3
TCU	24.15	120.68	.044	3
CHY	23.50	120.42	.044	3
ALS	23.51	120.81	.208	3
TAI	23.00	120.20	.013	3
PNG	23.57	119.56	.013	3
KAU	22.57	120.31	.022	3
HEN	22.01	120.74	.089	3
ILA	24.77	121.75	.013	3
HWA	23.98	121.61	.013	3
CHK	23.10	121.37	.013	3
TTN	22.75	121.15	.013	3
TAW	22.36	120.90	.013	3
LAY	22.04	121.55	.013	3
NCU	24.97	121.19	.013	3
YUS	23.48	120.95	.208	3
PCY	25.63	122.07	.013	3
SML	23.88	120.90	.026	3
NST	24.63	121.00	.013	3
WSF	23.64	120.22	.013	3
WTC	23.86	120.28	.013	3
SCL	23.18	120.19	.026	3
SGS	23.08	120.58	.104	3
SGL	22.73	120.49	.052	3
ENA	24.43	121.74	.013	3
ESL	23.81	121.43	.104	3
ENT	24.64	121.57	.052	3
NSY	24.42	120.76	.013	3
EHY	23.51	121.32	.013	3
WNT	23.88	120.68	.013	3
WGK	23.69	120.56	.013	3
WTP	23.25	120.61	.026	3
STY	23.16	120.76	.052	3
EGS	24.84	121.93	.013	3
NSK	24.68	121.36	.013	3
SSD	22.75	120.63	.013	3
EHC	24.27	121.73	.013	3
WDT	23.76	121.13	.013	3
SCZ	22.37	120.62	.013	3
TAI1	23.01	120.13	.022	3
TAP1	25.04	121.52	.800	3
TWA	24.98	121.58	.740	1
TWB1	25.01	121.99	.790	1
TWC	24.61	121.85	.780	1
TWD	24.08	121.60	.380	1
TWE	24.72	121.67	.960	1
TWF1	23.35	121.30	.740	1
TWG	22.82	121.07	.740	1
TWH	22.68	121.48	.480	2
TWI	22.07	121.50	.230	2
TWJ1	22.37	120.88	.230	2
TWK1	21.94	120.81	.470	1

Table 1. (Continued)

Station Code	Latitude Degree	Longitude Degree	Gain (count/mu)	Instrument Type*
TWL	23.27	120.49	.370	1
TWM1	22.82	120.42	.490	2
TWO1	23.57	120.59	.910	2
TWP	22.35	120.36	.230	2
TWQ	24.27	120.84	.550	1
TWQ1	24.35	120.77	.230	1
TWR	24.64	121.08	.770	1
TWS1	25.10	121.42	.220	1
TWT	24.25	121.18	.740	1
TWU	24.88	121.53	.380	1
TWX	25.20	121.66	.450	2
TWY	25.28	121.60	.250	1
TWZ	25.10	121.58	.220	1
TYC	23.90	120.86	.740	1

- * 1 - Analog transmission station of S-13 sensor.
 2 - Analog transmission station of L-4c sensor.
 3 - Digital transmission station of S-13 sensor.

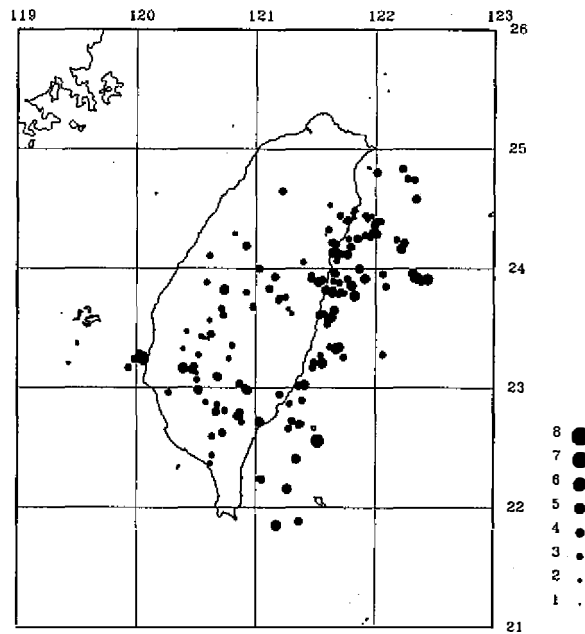


Fig. 2. The location map of 224 events used in this study. The size of solid circle represents the magnitude of earthquake.

where γ and n are the attenuation and geometrical spreading coefficients respectively; $R = \sqrt{\Delta^2 + h^2}$ (h is focal depth); C is a constant; and S is a site-dependent constant, which is affected by site effects and varies with station's magnification. Equation (2) can be related to the function $A_o(\Delta)$ shown in equation (1) as long as $A(\Delta) = 1$ mm at $\Delta = 100$ km.

The synthetic Wood-Anderson seismogram (SWAS) can be constructed from the short-period seismogram. The processing is explained as follows. First, the short-period seismogram is transformed into frequency domain; Second, the instrument response is removed to have ground displacement spectrum; then multiplied by a Wood-Anderson instrument response in frequency domain; Finally, the spectrum is transformed back into the time domain. It gives a SWAS (Bakun *et al.*, 1978). Figure 3 shows the examples of original short-period seismograms and SWAS. I measured three different types of zero-peak amplitude: (1) The maximum value from vertical component denoted as Z , and (2) The maximum value of the square-root of the vectorial sum of the peak amplitudes in the NS and EW components denoted as $H1 = \sqrt{HN^2(Max) + HE^2(Max)}$, and (3) The maximum value of the vectorized horizontal components denoted as $H2 = \sqrt{HN^2 + HE^2} | Max$.

To fit all measured peak amplitudes of SWAS (Z , $H1$, or $H2$) into equation (2) individually, I adopt the multiple linear regression analysis method by taking logarithm on both sides of equation (2) as

$$\log A(\Delta)R^n = \log C - \gamma R \log e + \log S \quad (3)$$

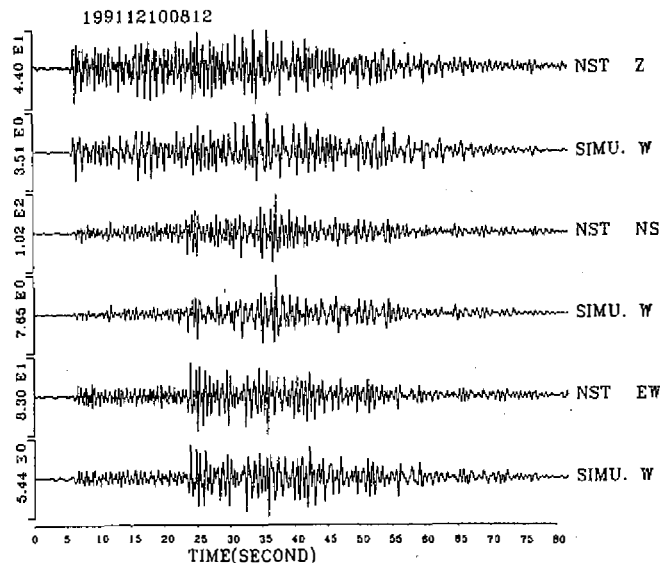


Fig. 3. Examples of simulated Wood-Anderson seismogram from short-period seismogram. The SWAS is plotted next to short-period seismogram.

The reduced amplitude in the left hand side of equation (3) has linear relationship with hypocentral distance R . In order to resolve C and S terms which both are constants representing different physical meanings, I applied an iteration technique. The term S is initialized as unit. The S term of each station is calculated by taking the averaged ratio of the observed value to the theoretical value after first iteration. Then, it can be used for the next iteration of regression analysis. The processing will be stopped by checking the ratio values as they approach 1 or the multiplication of all averaged ratio values approaching 1. Usually, it takes 3 or 4 iterations to make one of two conditions satisfied. The function $A_o(\Delta)$ is then formed by adjusting C to fit the scale used by Richter's (1935, 1958).

Assuming $n=0.833$ for the Lg wave propagation, Figure 4 shows the data points of reduced amplitude versus distance after 3 iterations of regression analysis. It is worth noting that a single linear equation can not fit the data points, especially at the short distance ($\Delta \leq 80$ km). The result indicates that the dominant wave is changed at different distance ranges. It is believed that shear wave has large amplitude at short distance while Lg wave is conspicuous at regional distance. It is consistent with the other observations (Bouchon, 1982; Hasegawa, 1983; Dwyer *et al.*, 1983; Campillo *et al.*, 1984; Shin and Herrmann, 1987). Considering this result and the depth distribution of earthquakes in the Taiwan area, the regression analysis is performed by three cases (1) Shallow earthquakes ($h \leq 35$ km) and long distance range ($\Delta > 80$ km); (2) shallow earthquakes ($h \leq 35$ km) and short distance range ($\Delta \leq 80$ km); and (3) deep earthquakes ($h > 35$ km)

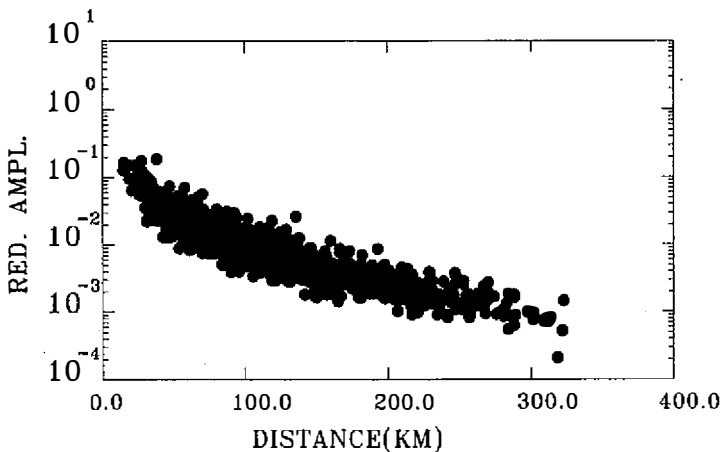


Fig. 4. Reduced amplitude vs distance for 224 earthquakes. It is obvious that a single linear line can not fit the data points.

3.1 Case 1

Totally, 102 earthquakes are used in this case. Each event has at least 10 recordings in the required distance range which is greater than 150 km. Using $n=0.833$ and $H 1$ to perform regression analysis, Figure 5 displays the data points of reduced amplitude vs. distance before (as open circles) and after (as solid circles) regression analysis. The linearity is more

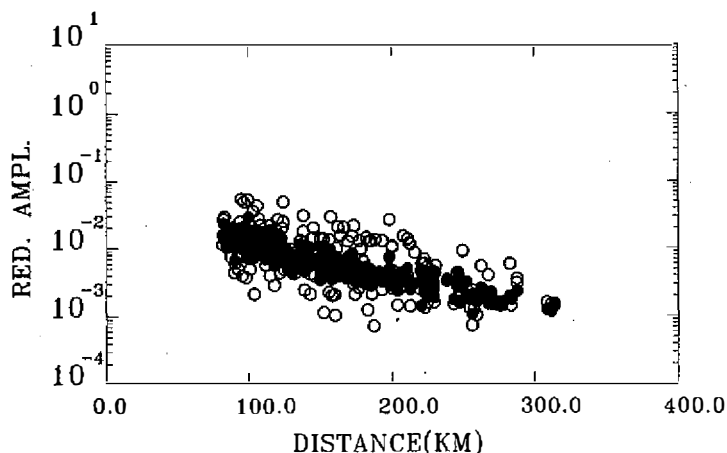


Fig. 5. The reduced amplitude of $H1$ for shallow earthquake in long distance range. Open circles represent the data points after one iteration of regression analysis: solid circles are the results of three iteration. The slope of solid circles on semi-log scale is 0.0026 which is equal to $\gamma = 0.0061 \text{ km}^{-1}$.

remarkable as regression is applied. The slope of 0.00261 is essentially implying the attenuation effects of the area. Therefore, the slope can be converted to have $\gamma = 0.0061 \text{ km}^{-1}$. To realize the variation of γ caused by using different kinds of peak amplitude, the data of $H2$ and Z are also taken for regression analysis. Figure 6 shows the distribution of reduced amplitude of $H2$ (as open circles) and Z (as solid triangles) individually.

The γ values of 0.006 km^{-1} and 0.0059 km^{-1} are obtained respectively. The same γ value tells that the propagation of seismic wave is similarly attenuated on the horizontal and vertical components. Results show that the $\log A_o(\Delta)$ function can be expressed as $-0.00261R - 0.83 \log R - 1.07$.

3.2 Case 2

Using recordings within short distance range, at least 4 recordings are required and the distance range greater than 50 km. There are 84 earthquakes meeting the requirement. Assuming $n=1.0$ of body wave propagation and $H1$ used, Figure 7 is the distribution of reduced amplitude with respect to the distance before (open circles) and after (solid circles) regression analysis respectively. The slope of 0.00716 is equal to $\gamma = 0.0165 \text{ km}^{-1}$. The same values are obtained as using either $H2$ or Z peak amplitude. Using the γ value, $\log A_o(\Delta)$ is in the form of $-0.00716R - \log R - 0.38$ in this case.

3.3 Case 3

There are 53 deep earthquakes ($h > 35 \text{ km}$) which are taken into account. For each of them, there are at least 10 recordings in the distance range greater than 150 km. Using $n=0.833$ and $H1$, Figure 8 is the reduced amplitude distribution before (open circles) and

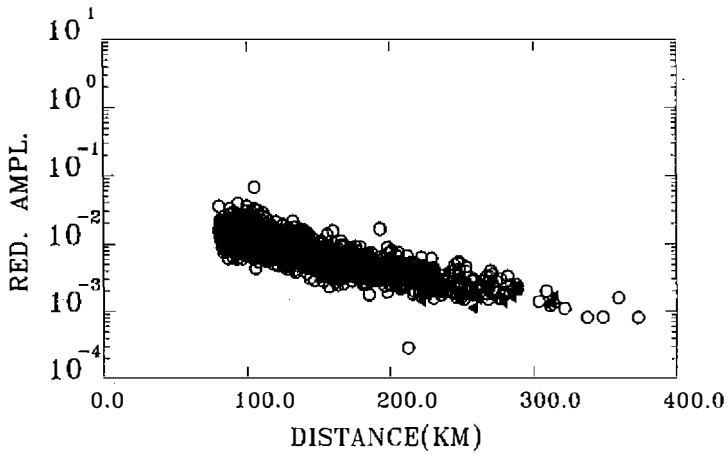


Fig. 6. The reduced amplitude distribution of $H2$ (open circles) and Z (solid triangles) in long distance range. The γ values of 0.006 km^{-1} and 0.0059 km^{-1} are obtained respectively. The similar value of γ from $H1$, $H2$, and Z indicates the same average path effects of seismic wave at all components for Taiwan area.

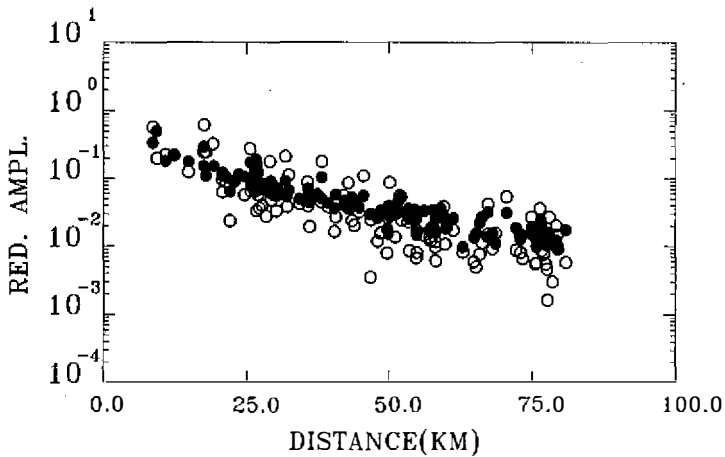


Fig. 7. The same notation as Figure 5 while $H1$ selected in short distance. The slope of solid circles is 0.00716 equating to $\gamma = 0.0165 \text{ km}^{-1}$.

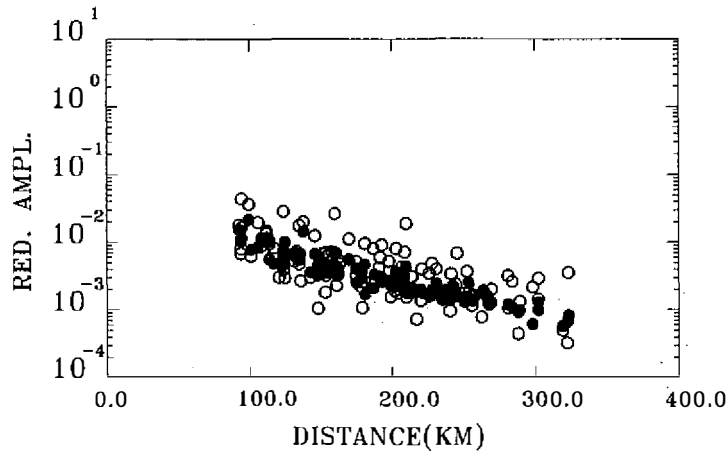


Fig. 8. The distribution of reduced amplitude. The $H1$ data of deep earthquakes are used, and the notations are the same as Figure 5. The slope of 0.00326 equals to $\gamma = 0.0075 \text{ km}^{-1}$.

after (solid circles) regression analysis respectively. The slope in the Figure 8 of solid circles is 0.00326 and equals to $\gamma = 0.0075 \text{ km}^{-1}$. Therefore, the $\log A_o(\Delta)$ function can be expressed by $-0.00326R - 0.83 \log R - 1.01$.

4. DISCUSSION AND CONCLUSIONS

Applying the multiple regression analysis for SWAS, a revised distance correction term for local magnitude is derived. The new $\log A_o(\Delta)$ function can be expressed as followings:

$$\log A_o(\Delta) = \begin{cases} -0.00716R - \log R - 0.39 & (0 \text{ km} < \Delta \leq 80 \text{ km}) \\ -0.00261R - 0.83 \log R - 1.07 & (80 \text{ km} < \Delta) \end{cases}$$

for shallow earthquakes ($h \leq 35 \text{ km}$), and

$$\log A_o(\Delta) = -0.00326R - 0.83 \log R - 1.01$$

for deep earthquakes ($h > 35 \text{ km}$)

Figure 9 shows the comparison of $\log A_o(\Delta)$ curves. The circles represent the Richter's curve for southern California. The squares are the attenuation function obtained by Yeh *et al.* (1982) by SWAS of strong motion data of Taiwan area. The line is obtained in this study of assuming focal depth at 10 km representing the attenuation curve of shallow earthquakes. The results indicate that the attenuation of seismic waves at short distance in Taiwan area is greater than those in southern California, but slightly less at long distance. The result from Yeh *et al.* (1982) is only for reference since the selected strong motion data are too few to

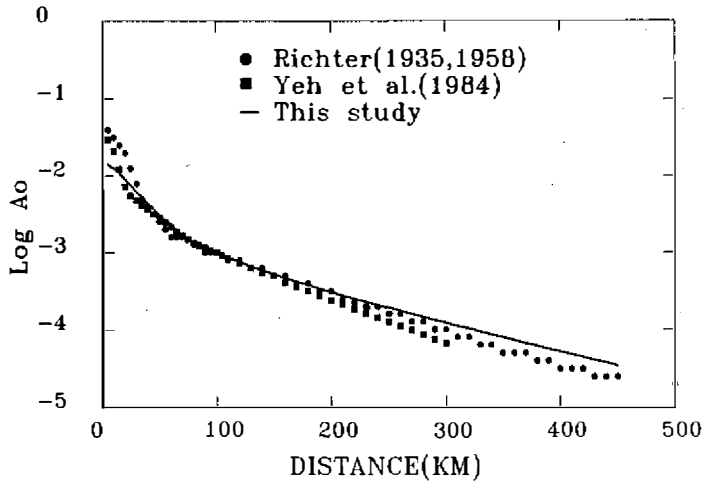


Fig. 9. Comparison of $\log A_0(\Delta)$ curves. The solid circles are from Richter (1935, 1958). The squares are the results of Yeh *et al.* (1984). The solid line is from this study assuming $h = 10$ km.

sample the whole area. Therefore, their attenuation curves cannot represent the full characteristics of the Taiwan area.

The attenuation coefficient (γ) can be related to the seismic quality factor, Q , if the form $Q = \pi f / \gamma U$, where f is the frequency of the wave, and U is its velocity. Thus, the γ value obtained from case 1 can be used to estimate the Q for Lg in the Taiwan area. The $Lg - Q$ is about 190 by assuming $U = 3.5$ km/sec and $f = 1.25$ Hz (the natural frequency of Wood-Anderson seismograph). Similarly, the shear wave Q of 165 can be calculated by assuming the shear velocity of 3.3 km/sec. All these results are consistent with the average Q values obtained by previous works for the Taiwan area (Chang and Yeh, 1983; Wang, 1988; Wang and Liu, 1990; Shin *et al.* 1987).

Using the $\log A_0(\Delta)$ curve developed in this study, the local magnitudes are recomputed by using $H1$ denoted as $M_L(H1)$, $H2$ as $M_L(H2)$, Z as $M_L(Z)$ of SWAS for 224 earthquakes. Figures 10a and 10b show the comparison of $M_L(H1)$ versus $M_L(H2)$ and $M_L(H1)$ versus $M_L(Z)$ respectively. It appears that the same magnitude values are obtained no matter the $H1$ or $H2$ used. On the other hand, the local magnitude calculated from Z is smaller than those from $H1$ or $H2$ by a factor of 0.5 magnitude unit. It turns out that the average ratio of horizontal peak amplitude to vertical peak amplitude is approximately 3.

The difference of local magnitude calculation by applying the Richter's $\log A_0(\Delta)$ ($M_L(\text{old})$) and the $\log A_0(\Delta)$ of this study ($M_L(\text{new})$) is shown as open circles in Figure 11. The data points include all events occurring in the Taiwan area from Sep. 1991 to Feb. 1992 and can be fitted by the regression line of

$$M_L(\text{new}) = 0.97M_L(\text{old}) + 0.12 \quad (4)$$

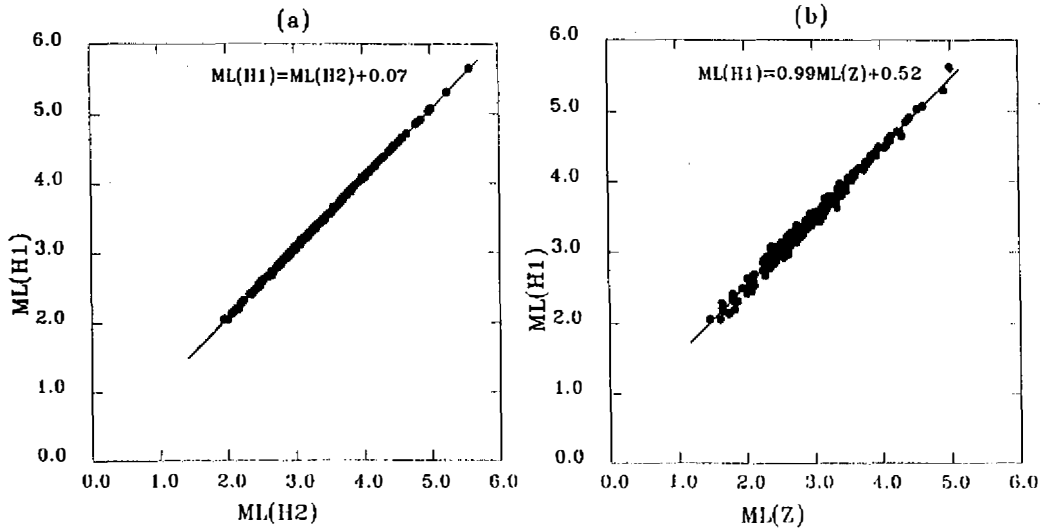


Fig. 10. (a) $M_L(H1)$ vs $M_L(H2)$, (b) $M_L(H1)$ vs $M_L(Z)$. The linear relationships are written in figure respectively.

Some data points deviate from this line and showing a underestimation of magnitude by using Richter's $\log A_0(\Delta)$. Taking the shallow earthquakes only (solid circles), they display a good linear trend as $M_L(\text{new}) = 0.97 M_L(\text{old}) + 0.09$. It indicates that the data points which deviate from the main trend of data points in Figure 11 are mostly for deep earthquakes.

Since 1973, the duration of earthquake signals recorded on seismogram has been used by the TTSN to determine magnitude (M_D) in the form

$$M_D = -0.87 + 2.00 \log D + 0.0035\Delta \quad (5)$$

obtained by Lee *et al.*, (1972) from southern California earthquakes, where D is total duration time in second. The M_D for the Taiwan earthquakes can be related to M_L in the form (Yeh and Hsu, 1985):

$$M_L = 0.94M_D + 1.04 \pm 0.28 \quad (6)$$

It is noted that M_L in equation (6) was determined from the $\log A_0(\Delta)$ values obtained by Yeh *et al.* (1982). In order to establish a unique magnitude scale, it is necessary to compare the M_D with the M_L of this study. Using the same data set, there are 221 earthquakes whose duration magnitudes were determined by the TTSN. Figure 12 shows the data points of M_L vs M_D . The relationship is in the form

$$M_L = 1.12M_D + 0.03 \pm 0.21 \quad (7)$$

and shown by a solid line in the figure. The dashed line is from equation (6). Obviously, equation (6) gives an overestimated M_L values comparing to equation (7), especially for the magnitude of earthquakes smaller than 5.6.

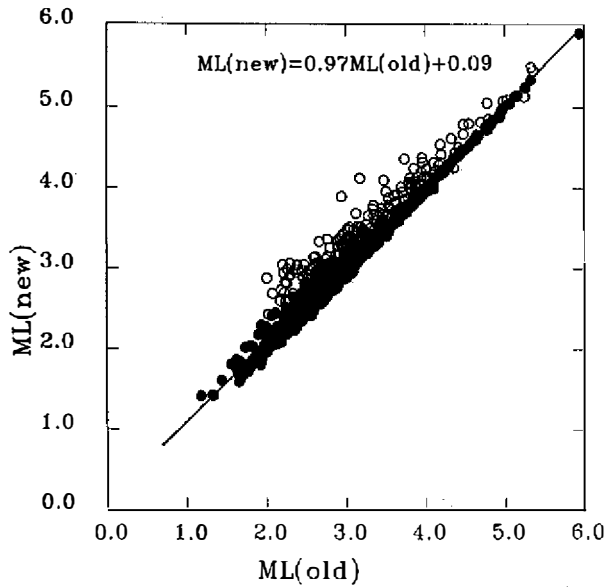


Fig. 11. The comparison of local magnitude using $\log A_0$ of this study (denoted as $M_L(\text{new})$) and Richter's $\log A_0$ (denoted as $M_L(\text{old})$) (1935, 1958). The open circles are the magnitude calculated from 224 earthquakes, the solid circles belong to shallow earthquakes only.

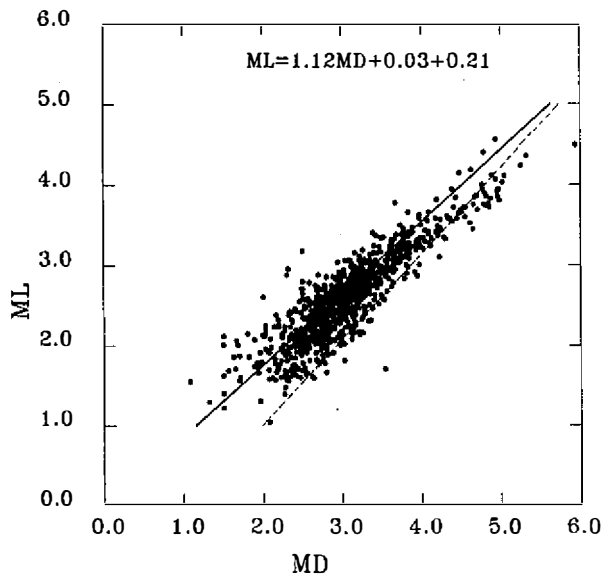


Fig. 12. The comparison of M_L and M_D of TTSN. A new relationship is developed written in the figure. The dashed line represents previous results of Yeh and Hsu (1985).

The M_L calculated by the data of accelerogram is important as the earthquake is large enough to cause the clip of the most of short-period seismograms. Because a large amount of triggered accelerograms can be used to calculate magnitude and the averaged value of magnitude will be more reasonable. In the period of Aug. 1991 to Jun. 1992, there are 28 earthquakes which triggered more than 3 strong motion accelerographs of CWBSN. Table 2 lists the parameters of all earthquakes. The strong motion data are used to simulate Wood-Anderson seismograms. The M_L magnitude (denoted as $M_L(\text{acc})$) of one event can be obtained by averaging all $M_L(\text{acc})$ values of the event while the individual magnitude is calculated by applying the attenuation function obtained in this study. Figure 13 shows the comparison of M_L magnitude from short-period seismogram to $M_L(\text{acc})$. A bisection line can be fitted to the data with standard error of 0.2 unit of magnitude. The scattering of data points in Figure 13 is due to small number of strong motion data comparing to the short-period data. However, it suggests that a compatible magnitude can be obtained if we use strong motion data.

Table 2. Earthquake parameters.

Date			Time			Location		Depth km	ML	
year	mo	dd	hh	mm	sec	Latitude Deg. Min.	Longitude Deg. Min.			
1991	8	26	10	18	44.74	24	2.32	121 35.22	22.87	4.84
1991	8	29	7	40	40.39	24	3.63	121 34.52	19.30	4.50
1991	9	9	20	57	52.21	22	43.55	120 55.44	1.41	4.77
1991	9	30	9	44	43.68	22	36.30	121 25.60	18.81	5.94
1991	9	30	17	31	12.94	23	46.27	121 28.88	2.41	4.95
1991	10	1	13	23	45.11	23	50.84	121 48.77	19.64	4.97
1991	10	12	5	8	40.46	22	52.14	121 26.13	23.34	5.33
1991	10	18	3	52	9.12	23	46.64	121 45.26	11.52	5.02
1991	11	3	4	17	20.51	23	27.70	121 35.84	35.27	5.03
1991	11	5	9	36	37.50	24	8.08	121 38.44	25.15	4.65
1991	11	21	16	53	2.08	23	15.75	120 3.77	6.90	4.41
1991	11	25	10	29	11.33	23	9.56	121 40.97	33.62	4.98
1991	12	2	6	14	15.72	23	10.83	121 41.83	35.03	5.36
1991	12	21	22	9	22.08	23	52.31	121 34.10	20.32	4.61
1991	12	24	2	51	43.47	23	10.95	120 43.63	7.60	4.94
1991	12	31	4	47	35.00	24	7.28	121 45.58	27.84	4.87
1992	2	4	10	5	28.12	23	9.84	120 23.82	15.72	4.67
1992	3	4	19	2	25.84	23	47.13	121 45.21	7.99	4.89
1992	3	21	3	11	59.29	23	59.91	121 36.54	26.76	5.05
1992	4	2	1	39	42.75	24	6.84	121 42.45	24.29	4.98
1992	4	19	18	32	20.75	23	50.43	121 34.47	8.07	5.57
1992	4	20	2	20	18.44	23	48.61	121 32.97	25.05	4.93
1992	4	20	16	16	38.80	24	27.05	120 42.86	8.80	5.19
1992	4	24	11	49	13.33	23	48.63	121 36.58	.77	5.24
1992	5	1	4	31	8.07	23	45.53	121 31.98	4.06	4.96
1992	5	28	23	19	35.45	23	7.93	121 21.05	13.68	5.44
1992	5	31	13	16	47.94	23	49.56	121 33.08	20.83	4.61
1992	6	8	4	58	7.20	23	58.44	121 38.14	23.08	4.01

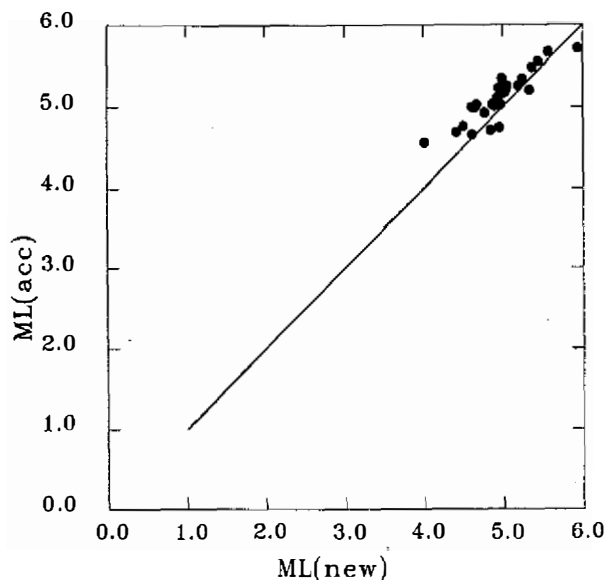


Fig. 13. M_L vs $M_L(\text{acc.})$. The data can be fitted with a line of slope one. The scatter data are due to the $M_L(\text{acc.})$ is averaged by the lower number of data since the strong motion data are triggered type.

Acknowledgments This research was sponsored by the National Science Council under contract NSC81-0202-M-052-01. The author thanks his colleagues at Seismological Observation Center, CWB for routine work and is also indebted to Mr. Z.S. Chang and Ms. M. Y. Ho for their help regarding data.

REFERENCES

- Bakun, W. H., and W. B. Joyner, 1984: The M_L scale in central California, *Bull. Seism. Soc. Am.*, **74**, 1827-1844.
- Bakun, W. H., S. T. Houck, and W. H. K. Lee, 1978: A direct comparison of 'synthetic' and actual Wood-Anderson seismogram, *Bull. Seism. Soc. Am.*, **68**, 1199-1202.
- Bouchon, G. A., 1982: The complete synthesis of seismic crustal phases at regional distances, *J. Geophys. Res.*, **87**, 1735-1741.
- Chang, L. S., and Y. T. Yeh, 1983: The Q value of strong ground motions in Taiwan, *Proc. Geol. Soc. China*, **32**, 339-353.
- Campillo, M., M. Bouchon, and B. Massinon, 1984: Theoretical study of the excitation, spectral characteristics, and geometrical attenuation of regional seismic phases, *Bull. Seism. Soc. Am.*, **74**, 79-90.

- Chavez, D. E., and K. F. Priestley, 1985: M_L observations in the Great basin and M_o versus M_L relationships for the 1980 Mammoth lakes, California, earthquake sequence, *Bull. Seism. Soc. Am.*, **75**, 1583-1598.
- Dwyer, J. J., R. B. Hermann, and O. W. Nuttli, 1983: Spatial attenuation of the Lg wave in the Central United States, *Bull. Seism. Soc. Am.*, **73**, 781-796.
- Hasegawa, H. S., 1983: Lg spectral of local earthquakes recorded by the Eastern Canada Telemetered Network and spectral analysis, *Bull. Seism. Soc. Am.*, **73**, 1041-1062.
- Lee, W. H. K., R. E. Bennett, and K. I. Meagher, 1972: A method of estimating magnitude of local earthquakes from signal duration, U.S. Geol. Surv. Open File Rept., 28 pp.
- Richter, C. F., 1935: An instrumental magnitude scale, *Bull. Seism. Soc. Am.*, **25**, 1-32.
- Richter, C. F., 1958: Elementary Seismology, W.H. Freeman and Co., San Francisco, California, 758 pp.
- Shin, T. C., and R. B. Herrmann, 1987: Lg attenuation and source studies using 1982 Miramichi data, *Bull. Seism. Soc. Am.*, **77**, 384-397.
- Shin, T. C., W. J. Su, and P. L. Leu, 1987: Coda Q estimates for Taiwan area, *Bull. Geophys.*, *NCU*, **27/28**, 111-118.
- Wang, C. Y., 1988: Calculations of Q_s and Q_p using the spectral ratio method in the Taiwan area, *Proc. Geol. Soc. China*, **31**, 81-89.
- Wang, J. H., and K. S. Liu, 1990: Azimuth variation of coda Q in northern Taiwan, *Geophys. Res. Lett.*, **17**, 1315-1318.
- Yeh, Y. T., and P. S. Hsu, 1985: Catalog of earthquakes in Taiwan from 1644 to 1984, *Inst. Earth Sci., Acad. Sin.*, Taipei.
- Yeh, Y. T., and G. B. Ou, and C. C. Lin, 1982: Determination of local magnitude scale for Taiwan, *Bull. Inst. Earth Sci., Acad. Sin.*, **2**, 37-48.